Bragg angle illumination on triple-layer grating for two-branch splitter

XU HUANG[1], BO WANG[1,2,*], RUIJUN LIU[1], XUANTONG SHI[1], GUOYU LIANG[1], YUQING XU[1], YONGYUAN HUANG[1]
[1]*School of Physics and Optoelectronic Engineering, Guangdong University of Technology, Guangzhou 510006, China*
[2]*Guangdong Provincial Key Laboratory of Sensing Physics and System Integration Applications, Guangdong University of Technology, Guangzhou, 510006, China*

A novel triple-layer structure grating for a two-branch splitter is proposed, which can obtain the 50/50 output with the polarization-independent property. Based on the simplified modal method and rigorous coupled-wave analysis, the parameters of the grating can be obtained. With optimized grating parameters, the efficiencies of TE polarization in the 0th and -1st orders are 49.56% and 49.45%, respectively, and the efficiencies of TM polarization in the 0th and -1st orders are 49.26% and 49.20%, respectively. Moreover, such a triple-layer grating has broad angular bandwidths for both TE and TM polarizations and a wide bandwidth of incident wavelength for TE polarization.

(Received December 11, 2023; accepted June 5, 2024)

Keywords: Triple-layer grating, Two-branch splitter, 50/50 output, Wide bandwidth

1. Introduction

With the development of micro-nano processing technology, sub-wavelength gratings (grating periods smaller than the wavelength of the incident light wave) are now small in size, compact in structure, and easy to integrate [1-4]. Due to their special polarization characteristics, two-branch splitters based on grating structures have attracted more and more attention from researchers [5-10]. A two-branch splitter can separate the transmission polarized light into two diffraction orders with good splitting ratio uniformity, which are widely used in optical systems such as optical communication [11, 12], optical detection [13, 14] and optical interconnection networks [15, 16].

Since the period of the sub-wavelength grating is smaller than the wavelength of the incident light wave, the assumptions of traditional scalar diffraction theory [17, 18] are invalid. It can only be analyzed by using the equivalent medium theory or the vector diffraction theory [19, 20]. The vector diffraction theory has been widely used and mainly includes rigorous coupled-wave analysis (RCWA) [21, 22], modal method (MM) [23, 24], finite element method (FEM) [25], and finite-difference time-domain method (FDTD) [26].

Wang et al. presented the splitter control by an embedded two-layer grating, which offered an effective guide to design grating-based splitter with a wide bandwidth for the incident wavelength [27]. Li et al. proposed a two-branch connecting-layer-based sandwiched splitter grating that had bandwidths of the incident wavelength of 227 nm for TE polarization and 63 nm for TM polarization [28].

In this paper, we introduce a novel transmission grating with a triple-layer structure that can be used as a two-branch splitter to achieve 50/50 output. By using rigorous coupled-wave analysis, the parameters of a high-efficiency grating can be obtained. The physical mechanism within the grating can be explained through the application of the simplified modal method. Besides, the parameters are verified using the finite element method. As far as we are aware, this is the first time that a triple-layer structural grating under Littrow mounting has been used as the basis for a two-branch splitter. Most importantly, our proposed grating can achieve higher efficiency, a wider incident angular bandwidth, and wider bandwidths of the incident wavelength for both TE and TM polarizations when compared to the sandwiched grating [28]. Based on its advantages, it is believed that such a triple-layer grating for a two-branch splitter could be used in the future as a highly sensitive device for a variety of optical detection applications, such as exosome detection in biomedical testing [29, 30].

2. Structure and theory

Fig. 1 depicts the schematic of the two-branch splitter grating with a triple-layer structure. Fused-silica is used as the material for the grating substrate. The grating rectangular ridge is comprised of three kinds of dielectric materials. The material of the first layer is Ta_2O_5, with a

refractive index of n_1=2.00. The material of the second layer is HfO_2, with a refractive index of n_2=1.878. The material of the third layer is SiO_2, with a refractive index of n_3=1.45. The grating rectangular ridge has layers with thicknesses of h_1, h_2, and h_3, in that order. The grating groove between the grating ridge is filled with air, which has a refractive index of n_0=1.00. Besides, the grating period is defined as d, and the width of the grating ridge is b, so the duty cycle is $f=b/d$. In this work, an incident light with a wavelength of λ=1550 nm from air is incident at a Bragg angle of $\theta_i = \sin^{-1}(\lambda/(2d))$ on a triple-layer grating.

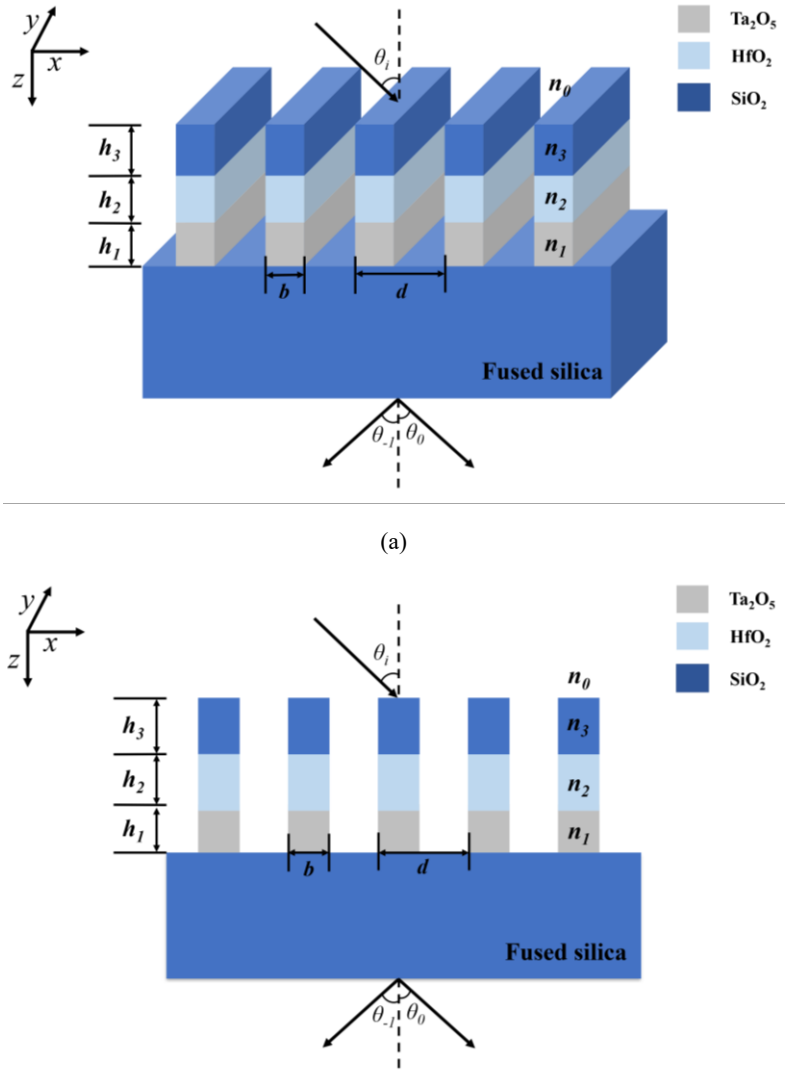

Fig. 1. Schematic diagram of the two-branch splitter grating with a triple-layer structure: (a) 3-D view and (b) 2-D view (color online)

The simplified modal method can reasonably explain the coupling mechanism of the triple-layer transmission grating. Grating modes are excited as incident light propagates through the grating, and each grating mode receives nearly the same amount of energy from the incident light. The eigenfunction of the incident light in the grating regions can be described as [31]:

$$F\left(n_{eff}^2\right) = cos(\frac{2\pi d \sin\theta}{\lambda}), \tag{1}$$

where n_{eff} is the effective refractive indices. When there are only two modes of 0 and 1 in the grating, the grating period should meet the conditions [31]:

$$\frac{\lambda}{2} < d < \frac{3\lambda}{2n}, \tag{2}$$

where n = 1.45 is the refractive index of the substrate material. Due to the asymmetry between the two modes, the effective refractive indices n_{eff} of mode 0 and mode 1

are different. Through rigorous calculations, the duty cycle of f = 0.55 and the period of d=1260 nm can be obtained. Thus, the effective indices in each layer can be calculated with the different refractive index of the grating ridge. The effective indices in the three grating layers for TE and TM polarizations are listed in Table 1.

Table 1. Effective indices in three grating layers with f=0.55, d=1260 nm and λ=1550 nm

Mode	n_{eff}^{1TE}	n_{eff}^{1TM}	n_{eff}^{2TE}	n_{eff}^{2TM}	n_{eff}^{3TE}	n_{eff}^{3TM}
0	1.8351	1.7306	1.7090	1.6026	1.2654	1.1760
1	1.3720	1.1633	1.2653	1.1188	0.9723	0.9837

According to the simplified modal method, the diffraction efficiency can be determined mainly by the accumulated phase difference $\Delta\varphi$ of the two modes. Hence, efficiency can be expressed by

$$\eta_0 = \cos^2\frac{\Delta\varphi}{2} \tag{3}$$

$$\eta_{-1} = \sin^2\frac{\Delta\varphi}{2}. \tag{4}$$

In order to obtain 50/50 output for TE polarization and TM polarization, the accumulated phase differences of the TE polarization and TM polarization after transmission through the grating should meet the conditions:

$$\Delta\varphi^{TE} = \frac{2\pi}{\lambda}[\left(n_{0eff}^{1TE} - n_{1eff}^{1TE}\right)h_1 + \left(n_{eff0}^{2TE} - n_{eff1}^{2TE}\right)h_2 + \left(n_{0eff}^{3TE} - n_{1eff}^{3TE}\right)h_3] = (2p+1)\frac{\pi}{2} \tag{5}$$

$$\Delta\varphi^{TM} = \frac{2\pi}{\lambda}[\left(n_{0eff}^{1TM} - n_{1eff}^{1TM}\right)h_1 + \left(n_{eff0}^{2TM} - n_{eff1}^{2TM}\right)h_2 + \left(n_{0eff}^{3TM} - n_{1eff}^{3TM}\right)h_3] = (2q+1)\frac{\pi}{2} \tag{6}$$

with p and q are arbitrary integers, and n_{keff}^{iTx} is the effective indices of different Tx polarization of the mode k in layer i. Based on rigorous calculation, the thickness of h_1 is 0.28 μm. Therefore, the approximate thicknesses of h_2 and h_3 can be obtained by solving the equations (5) and (6). Fig. 2 displays the four distinct lines of the triple-layer grating for TE and TM polarizations based on equations (5) and (6). There are two intersection points in the figure. To reduce the difficulty of manufacturing, we select the intersection point where p and q are zero, which shows h_3=0.258 λ=0.40 μm and h_2=0.202 λ=0.31 μm. It means that the grating parameters can be optimized near such a point to obtain a two-branch splitter with 50/50 output.

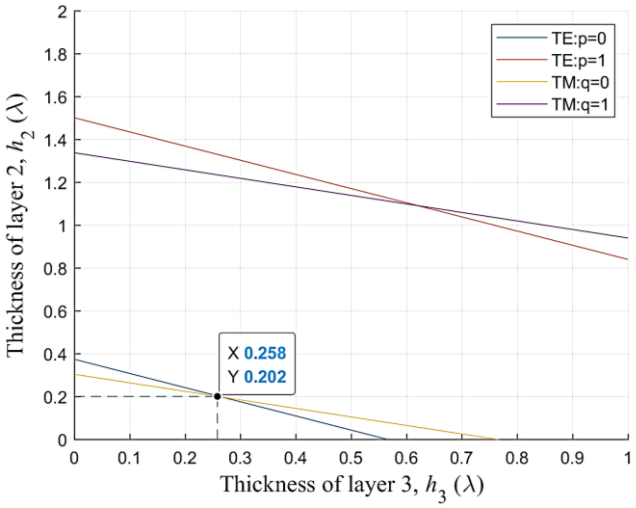

Fig. 2. The four different lines of the triple-layer grating for TE and TM polarizations based on Eqs. (5) and (6) for the duty cycle of 0.55 and period of 1260 nm (color online)

To enhance the accuracy of efficiency calculations, RCWA can be used in numerical calculations. Fig. 3 shows the efficiency's ratio between the 0th and -1st orders versus the thicknesses of layer 3 and layer 2. As can be seen from Fig. 3 (a) and Fig. 3 (b), the efficiency's ratios of 1.00222 and 1.00123 can be achieved for TE polarization and TM polarization when the thicknesses of h_3 and h_2 are 0.38 μm and 0.32 μm, respectively. Fig. 6 depicts the efficiency versus the thicknesses of layer 3 and layer 2. When the thicknesses of h_3 and h_2 are set to 0.38 μm and 0.32 μm, respectively, high efficiencies of 49.56% and 49.45% can be achieved for TE polarization in the 0th order and the -1st order, respectively, and high efficiencies of 49.26% and 49.20% can be achieved for TM polarization in the 0th order and the -1st order, respectively. These efficiencies for both TE and TM polarizations are more than 49% with the optimized parameters, surpassing those of the transmission two-branch splitter grating under Littrow mounting [27, 28]. The optimized parameters of the triple-layer structure grating are listed in Table 2. In addition, with the optimized parameters, the phase differences of the TE and TM polarizations can be calculated according to equations (5) and (6). By calculation, the phase differences for the TE and TM polarizations are $\Delta\varphi^{TE}$= 1.6216 and $\Delta\varphi^{TM}$= 1.7197, respectively, indicating that they approximately match π/2.

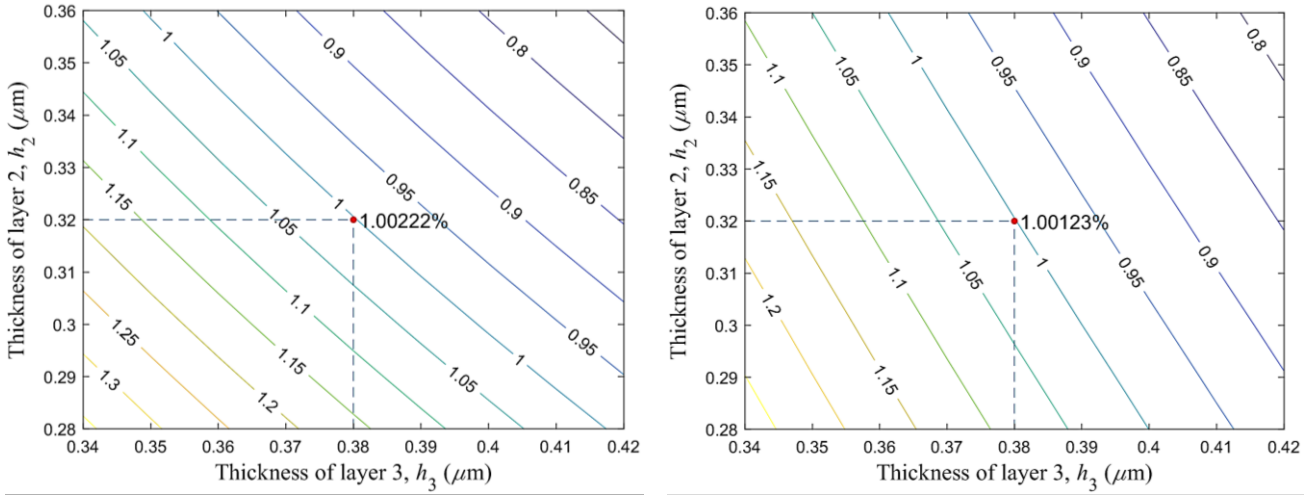

(a) (b)

Fig. 3. The efficiency's ratio between the 0th and -1st orders versus the thicknesses of layer 3 and layer 2 with λ=1550 nm, d=1260 nm, f=0.55, h_1=0.28 μm: (a) TE polarization and (b) TM polarization (color online)

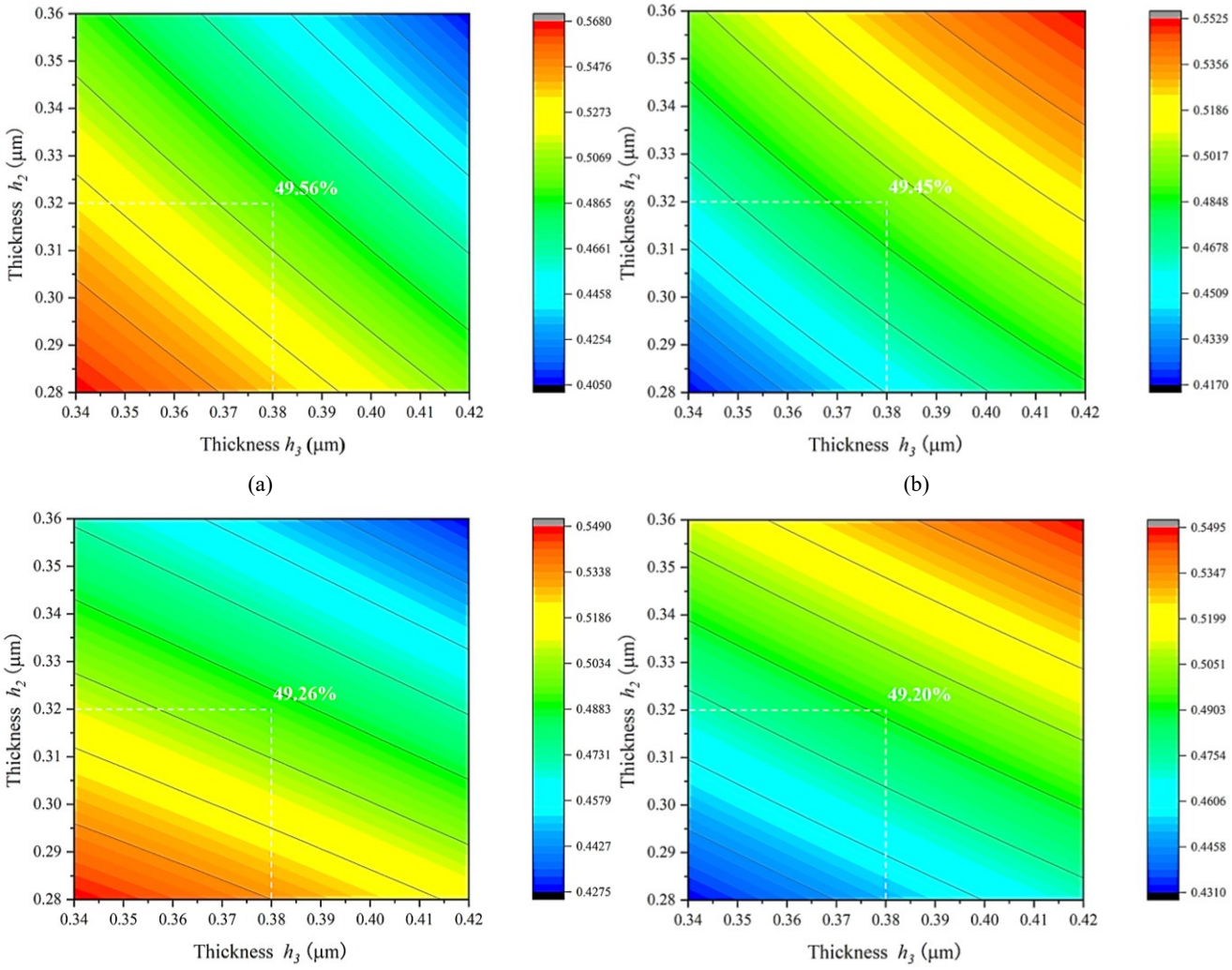

(a) (b)

(c) (d)

Fig. 4. Efficiencies in orders for the grating versus thicknesses of layer 3 and layer 2 with λ=1550 nm, d=1260 nm, f=0.55 and h_1=0.28 μm: (a) efficiency of 0th order for TE polarization, (b) efficiency of -1st order for TE polarization, (c) efficiency of 0th order for TM polarization, (d) efficiency of -1st order for TM polarization (color online)

Table 2. The optimized parameters of the triple-layer structure grating

d	f	λ	h_1	h_2	h_3
1260 nm	0.55	1550 nm	0.28 μm	0.32 μm	0.38 μm

In addition, based on the optimized parameters, using FEM can also determine the efficiencies of TE and TM polarizations in the 0th order and the -1st order. The results of two theories used to calculate the efficiency are listed in Table 3.

Table 3. The efficiencies of grating under the optimized parameters based on RCWA and FEM

Theory	η_0^{TE} (%)	η_{-1}^{TE} (%)	η_0^{TM} (%)	η_{-1}^{TM} (%)
RCWA	49.56	49.45	49.26	49.20
FEM	49.57	49.44	49.24	49.11

Fig. 5 depicts the normalized electric field distribution of the triple-layer structure grating under Bragg incidence for both TE and TM polarizations. The electric field distribution map shows the process of the light wave propagation in the grating. As depicted in Figs. 5 (a) and (b), such a two-branch splitter based on a triple-layer structure grating has good splitting ratio uniformity for both TE and TM polarizations.

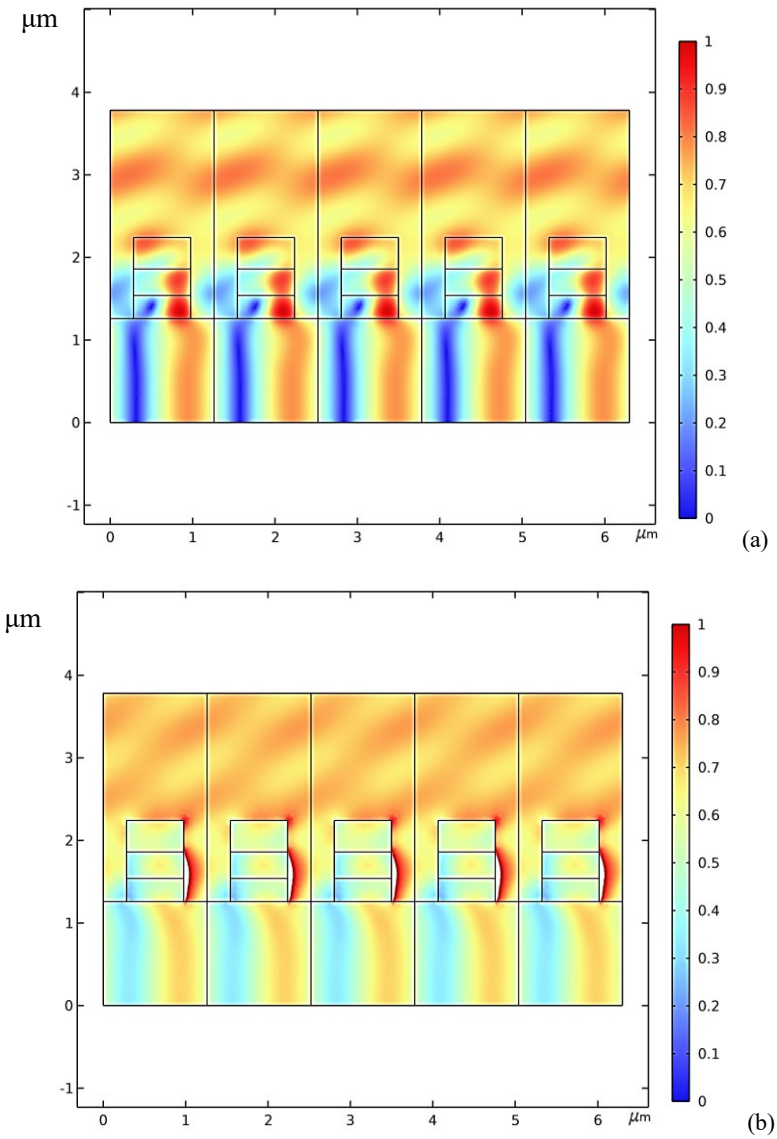

Fig. 5. Normalized electric field distribution diagram of the triple-layer structure grating under Bragg incidence: (a) TE polarization and (b) TM polarization (color online)

3. Discussions

After accurately determining the grating parameters using RCWA, it is essential to consider the diffraction properties of the grating in practical applications. Fig. 6 depicts the diffraction efficiency versus incident angle for TE and TM polarizations. When the incident angle is in the range of 26.7-54.2° (bandwidth of 27.5°), the diffraction efficiencies of both TE and TM polarizations in the 0th order and the -1st order can be kept at more than 45%. This indicates that such a two-branch splitter grating can retain a high level of splitting ratio uniformity for TE and TM polarizations over a broad angular bandwidth.

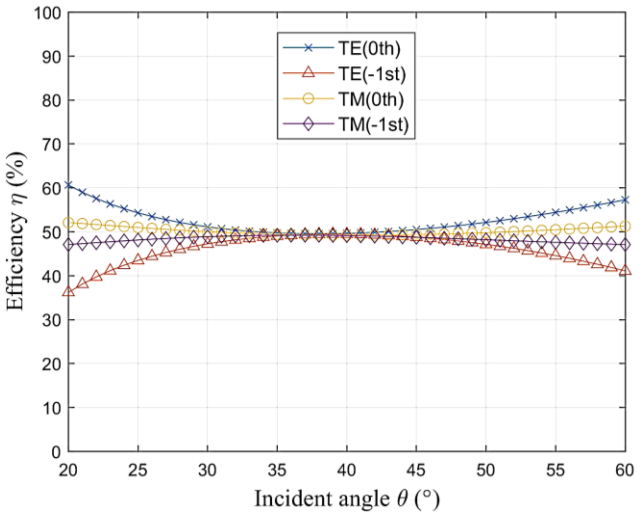

Fig. 6. The efficiency versus the incident angle with d=1260 nm and f=0.55 (color online)

Fig. 7 shows the diffraction efficiency versus incident wavelength for TE and TM polarizations. As can be seen, the bandwidth of the incident wavelength for TE polarization outperforms that for TM polarization. For TM polarization, the efficiencies in the 0th order and the -1st order can exceed 45% within the wavelength range of 1506-1595 nm (bandwidth of 89 nm). For TE polarization, the efficiencies in the 0th order and the -1st order can exceed 45% within the wavelength range of 1414-1809 nm (bandwidth of 395 nm). Notably, the bandwidths of incident wavelength for both TE and TM polarizations of the triple-layer structure grating are much higher than the bandwidths of the sandwiched grating [28].

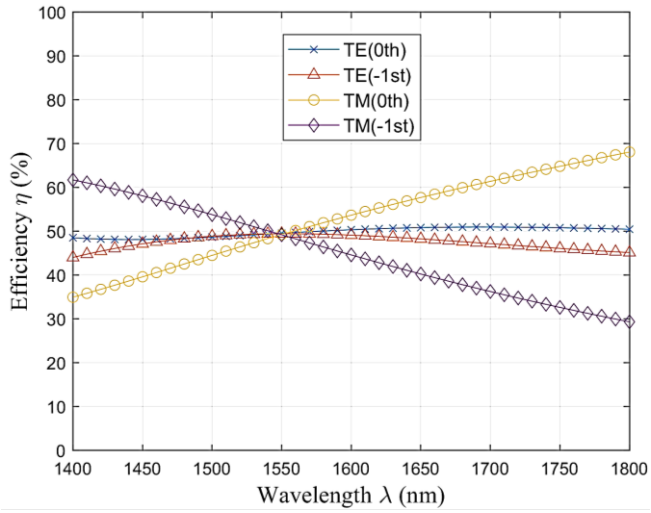

Fig. 7. The efficiency versus the incident wavelength with d=1260 nm and f=0.55 (color online)

Due to the fact that the duty cycle has an influence on transmission efficiency, the manufacturing tolerance of the grating needs to be considered in practical fabrication. Fig. 8 demonstrates the efficiency versus the duty cycle for TE and TM polarizations. Within the duty cycle range of 0.49 to 0.65, the efficiencies for TM polarization can surpass 45% in the 0th order and -1st order. Similarly, within the duty cycle range of 0.53 to 0.57, the efficiencies for TE polarization can exceed 45% in the 0th order and -1st order. Therefore, such a triple-layer structure grating exhibits a wide manufacturing tolerance for TM polarization.

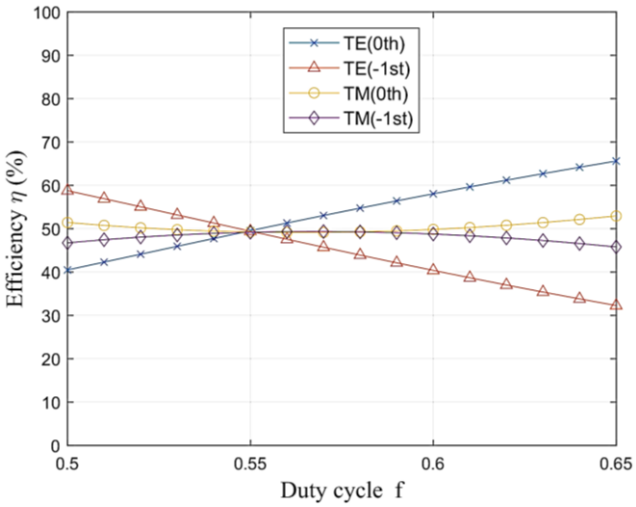

Fig. 8. The efficiency versus the duty cycle with d=1260 nm and λ=1550 nm (color online)

4. Conclusion

In conclusion, this paper presents a high-efficiency transmission grating with a triple-layer structure that exhibits a broad angular bandwidth and a wide bandwidth of the incident wavelength. The grating can function as a two-branch splitter to achieve 50/50 output with the polarization-independent property. Initially, the simplified modal method is employed to obtain the approximate thickness of the grating ridge. Subsequently, utilizing RCWA, the parameters of grating are optimized. With optimized grating parameters, efficiencies of 49.56% and 49.45% for TE polarization in the 0th and -1st orders can be achieved, respectively, while efficiencies of 49.26% and 49.20% for TM polarization in the 0th and -1st orders can be achieved, respectively. Besides, the finite element method is used to verify the parameters from RCWA. Furthermore, discussion on the grating diffraction properties is provided. It is demonstrated that good splitting ratio uniformity is exhibited when the incident angle is in the range of 34.6° to 49.4°. The diffraction efficiencies of TE polarization in the 0th and -1st orders can exceed 45% within the incident wavelength range of 1414 nm to 1809 nm, while those of TM polarization in the 0th and -1st orders can exceed 45% within the incident wavelength range of 1506 nm to 1595 nm. What's more, such a triple-layer structure grating exhibits a wide manufacturing tolerance for TM polarization. Therefore, based on these findings, it can be concluded that this proposed grating would be a promising element in numerous optical applications, including as a highly sensitive device for tumor-derived exosome detection.

Acknowledgements

This work is supported by the Natural Science Foundation of Guangdong Province (2024A1515012690).

References

[1] R. Sumi, N. D. Gupta, B. K. Das, IEEE Photon. **31**(17), 1449 (2019).
[2] Z. Cheng, J. Wang, Z. Yang, L. Zhu, Y. Yang, Y. Huang, X. Ren, Opt. Express **27**(23), 34434 (2019).
[3] Y. Zhou, Z. Guo, W. Zhou, S. Li, Z. Liu, X. Zhao, X. Wu, Nanotechnology **31**(32), 325501 (2020).
[4] Q. Qiao, H. Sun, X. Liu, B. Dong, J. Xia, C. Lee, G. Zhou, Micromachines **12**(11), 1311 (2021).
[5] B. Wang, L. Chen, L. Lei, J. Zhou, IEEE Photon. Technol. Lett. **25**(9), 863 (2013).
[6] B. Wang, H. Li, W. Shu, W. Li, L. Chen, L. Lei, J. Zhou, Mod. Phys. Lett. B **30**, 1550257 (2016).
[7] Z. Yin, Y. Lu, J. Yu, C. Zhou, Chin. Opt. Lett. **18**(7), 070501 (2020).
[8] Z. Xiong, B. Wang, X. Zhu, Y. Huang, L. Li, J. Hong, Y. Zhou, Optoelectron. Adv. Mat. **16**(5-6), 187 (2022).
[9] X. Zhu, B. Wang, Z. Xiong, Y. Huang, Optik **260**, 169049 (2022).
[10] H. Zou, B. Wang, J. Electromagn. Waves Appl. **37**(17), 1435 (2023).
[11] Q. Huang, W. Wang, W. Jin, K. S. Chiang, IEEE Photon. Technol. Lett. **31**(13), 1052 (2019).
[12] S. Hu, S. Du, J. Li, C. Gu, Nano Lett. **21**(4), 1792 (2021).
[13] M. A. Quiroz-Juárez, A. Perez-Leija, K. Tschernig, B. M. Rodríguez-Lara, O. S. Magaña-Loaiza, K. Busch, Y. N. Joglekar, R. J. León-Montiel, Photon. Res. **7**(8), 862 (2019).
[14] D. Feng, Y. Gao, X. Zhang, T. Zhu, R. Cao, Opt. Commun. **460**, 125198 (2020).
[15] Y. Wang, Y. Guo, H. Liao, Z. Li, F. Gan, C. Sun, J. Chen, ACS Photon. **5**, 1575 (2018).
[16] J. Ruan, Y. Gao, C. Song, P. Xu, W. Zhang, Y. Chen, X. Shen, Opt. Express **31**(20), 33091 (2023).
[17] J. A. Stratton, L. J. Chu, Phys. Rev. **56**(1), 99 (1939).
[18] C. J, Bouwkamp, Rep. Prog. Phys. **17**(1), 35 (1954).
[19] A. S. Marathay, J. F. McCalmont, J. Opt. Soc. Am. A **18**(10), 2585 (2001).
[20] J. Kim, Y. Wang, X. Zhang, J. Opt. Soc. Am. A **35**(4), 526 (2018).
[21] W. Lee, F. L. Degertekin, J. Lightw. Technol. **22**(10), 2359 (2004).
[22] M. Weismann, D. F. G. Gallagher, N. C. Panoiu, J. Opt. **17**(12), 125612 (2015).
[23] B. Wang, L. Chen, L. Lei, J. Zhou, Opt. Commun. **306**, 74 (2013).
[24] F. Yang, Y. Li, Opt. Express **23**(24), 31342 (2015).
[25] G. Bao, Z. Chen, H. Wu, J. Opt. Soc. Am. A **22**(6), 1106 (2005).
[26] A. K. Agrawal, A. Suchitta, A. Dhawan, IEEE Access **9**, 10136 (2021).
[27] B. Wang, H. Li, W. Shu, W. Li, L. Chen, L. Lei, J. Zhou, Superlattices Microst. **85**, 624 (2015).
[28] H. Li, B. Wang, Sci. Rep. **7**, 1309 (2017).
[29] H. Li, H. Wu, L. Lu, J. Zhang, X. Wang, W. Wang, A. Zheng, L. Liang, H. Sun, J. Zheng, H. Yuan, Z. Cao, Q. Yu, B. Yu, H. Wang, Adv. Opt. Mater. **12**(5), 2301670 (2024).
[30] H. Li, T. Huang, L. Lu, H. Yuan, L. Zhang, H. Wang, B. Yu, ACS Sens. **7**(7), 1926 (2022).
[31] I. C. Botten, M. S. Craig, R. C. Mcphedran, J. L. Adams, J. R. Andrewartha, Opt. Acta **28**(3), 413 (1981).

*Corresponding author: wangb_wsx@yeah.net